Highly Stable and Tunable n-Type Graphene Field-Effect Transistors with Polyvinyl Alcohol Films

Sungjin Kim[†], Pei Zhao[§], Shinya Aikawa[‡], Erik Einarsson[⊥], Shohei Chiashi[†], and Shigeo Maruyama[†,‖,*]

[†]Department of Mechanical Engineering, The University of Tokyo, 7-3-1 Hongo, Bunkyo-ku, Tokyo 113-8656, Japan

[§]Institute of Applied Mechanics, Zhejiang University, Hangzhou, Zhejiang 310027, China

[‡]Research Institute for Science and Technology, Kougakuin University, 2665-1 Nakano, Hachioji, Tokyo 192-0015, Japan

[⊥]Department of Electrical Engineering, University at Buffalo, The State University of New York, Buffalo, NY 14260, USA

[‖]National Institute of Advanced Industrial Science and Technology, 1-2-1 Namiki, Tsukuba, 305-8564, Japan

*Corresponding author. Phone: 81-3-5841-6421. Fax: 81-3-5800-6983. E-mail: maruyama@photon.t.u-tokyo.ac.jp

ABSTRACT

The intrinsic p-type behavior of graphene field-effect transistors (FETs) under ambient conditions poses a fundamental challenge for the assembly of complex electronic devices such as integrated circuits. In this work, we present a protocol of tunable n-type doping of graphene FETs *via* polyvinyl alcohol (PVA) coating. Using graphene grown by alcohol catalytic chemical vapor deposition, functionalization of the surface by this hydroxyl anion-rich polymer results in an evolution of the FETs from p-type to ambipolar or n-type even under ambient air condition. The doping level of graphene is strongly related to the PVA film coating parameters, such as solution concentration, hardening temperature and hardening time. This PVA coating proves to be a simple and stable approach to tuning the Dirac point and doping level of graphene, which is highly desirable and of great significance to the future graphene-based electronic devices.

KEYWORDS: chemical vapor deposition, graphene, n-type doping, field-effect transistor, polyvinyl alcohol thin film

Introduction

There are many advantages to using graphene for electronic and optoelectronic devices due to graphene's outstanding electrical, mechanical, and optical transparent properties.[1-3] Its many physical and electrical properties, such as extraordinarily high carrier mobility (up to 200,000 $cm^2V^{-1}s^{-1}$),[4] ballistic transport distance up to 1 μm,[5] half-integer quantum Hall effect,[6-7] and superior mechanical elasticity,[8] open up possibilities as a promising candidate to substitute silicon in the next generation of electronics. However, the full potential of graphene in the device industry is still restricted by several challenges. For example, it is crucial to open a bandgap in graphene to realize the ON- and OFF-states in electronic devices. Solutions to this challenge involve tailored nanoribbon structures,[9-12] bilayer graphene in the presence of a vertical electric field,[13-16] graphene nanomeshes,[17] etc. Furthermore, due to the fact that ambient conditions makes graphene behave as a p-type semi-metal,[18] we must adjust the positive and negative carrier concentrations by shifting the Fermi level away from its Dirac point in order so that the device can also behave as n-type and be assembled into circuits.[19-20] Several approaches to locally change the carrier density have been explored using different dopants, such as gases, alkali metals, polymers, heteroatom, photochemical, and so on.[18, 20-26] However, these approaches show disadvantages in device fabrication, such as difficulty in processing or patterning, or poor device stability, applicability, controllability and so on. For instance, potassium doping has led to the fabrication of n-type graphene field-effect transistors (FETs) and enabled the integration of more complex devices such as intra-graphene p-n junctions with different device functions.[27] Furthermore, such alkali dopants

suffer from immediate degradation upon exposure to air, making them inapplicable for n-type doping of graphene in practical device applications.

In this work, we present a protocol of tunable n-type doping of graphene by functionalizing the surface with a polyvinyl alcohol (PVA) film. Using high-quality graphene grown by alcohol catalytic chemical vapor deposition (ACCVD), functionalization of the graphene surface by this hydroxyl anion-rich polymer results in an evolution of the FETs from p-type to ambipolar or n-type. The doping level of graphene is strongly correlated with different treatment conditions of the PVA film, for instance, the polymer concentration. This PVA coating proves to be a simple and stable approach to tuning the Dirac point and doping level of graphene, and this environmentally free n-type doping enables us to fabricate more complex electronic devices such as p-n junction diodes, complementary inverters, and numerous complicated logic circuits.

Experimental Methods

The graphene used in our study was produced by ACCVD using a copper foil enclosure, as described in our previous work.[28] Briefly, the copper substrate was first cleaned by hydrogen chloride, acetone and isopropanol sequentially to remove the foil protection layer. To smooth the metal surface and remove metal oxides, the copper substrate was annealed at 1000 ^{o}C for 20 min in Ar/H_2 (3% H_2). The graphene growth was at 1000 ^{o}C with 10 sccm ethanol flow diluted by 300 sccm Ar/H_2, and the growth time was 10 min.[28] Uniform monolayer graphene was obtained on the inside surface of the copper enclosure. As to device fabrication, the source/drain electrodes were firstly patterned on a SiO_2/Si (600 nm) substrate using a standard photolithography process. The 40 nm/2 nm thick Pt/Ti electrodes were deposited in high vacuum condition using a thermal

evaporator (ULVAC, VPC-260F) with a quartz crystal thickness meter (ULVAC, CRTM-6000). As-grown graphene was then transferred using poly(methyl methacrylate) (PMMA) (average molecular weight ~950k, Sigma-Aldrich) 4% in anisole onto the substrate with predefined electrodes, similar to the process reported previously.[29] The PMMA layer was then removed by acetone, followed by annealing the device at 350 ^{o}C for 3 hours under vacuum condition. Subsequently, the second photolithography step was adopted to remove graphene film exclusive of the channel region between source and drain by exposing the substrate oxygen plasma (100 W, 100 Pa) for ~1 min.

The PVA solution was prepared by dissolving 1, 10, or 20 wt% PVA powder (average molecular weight ~1500, Wako) in distilled water. The polymer thin films were formed on the graphene channel by spin-coating the solution at 2000 rpm for 60 s, followed by baking at 60–150 ^{o}C for 10–30 min.

After the fabrication of pristine and polymer-coated graphene FETs, the devices were characterized using a semiconductor parameter analyzer system (Agilent 4156C) under air and vacuum condition, scanning electron microscopy (SEM, Hitachi, S-4800, acceleration voltage at 5 kV), and micro-Raman spectroscopy (Nanophoton Raman-11 system, Renishaw inVia system).

Results and discussion

Figure 1a presents the SEM image of as-grown graphene on the inside surface of a copper enclosure. The graphene film shows uniform high quality, as demonstrated by the scanning Raman map in Figure 1b. The number of active graphene layers was determined from the intensity ratio between the Raman G'- and G-bands ($I_{G'}/I_G$), which exhibits an average value of ~2. Only a small disorder band is visible in the Raman spectra (see Figure S1 in the Supporting Information), which

proves the high quality monolayer of graphene. Its full width at half maximum (FWHM) was 32–35 cm^{-1} in our as-grown graphene, consistent with the value reported for monolayer graphene.[30] Figures 1c and 1d illustrate the schematic and SEM image of our graphene FETs on silicon substrate with a bottom gate and a coated polymer film as dopants. So far PVA was formerly an encouraging material as polymer dielectrics in flexible devices or alignment layer in liquid crystal applications due to its high dielectric constant, good surface alignment effect, photosensitivity, and good resistance to damage by solvents involved in the lift-off process.[31, 32] We have examined the doping effect of the graphene devices with PVA coating by preparing an as-grown graphene on SiO_2/Si substrate and measuring its gate response to different polymer film conditions, such as annealing time, temperature, and polymer concentrations. The functionalization of the graphene surface by hydroxyl anion-rich polymers leads to the development of graphene from p-type to n-type or ambipolar. Here, doping by functional groups of adsorbed polymers on graphene presents a simple means of changing the doping level. Furthermore, we achieve n-type graphene FETs that are stable under air without keeping the graphene in a vacuum or an inert environment. This is discussed in more detail below.

We demonstrate that the adsorption of PVA on graphene results in a negative shift of the Dirac point. Similar phenomena were also reported for single-walled carbon nanotube FETs and graphene using poly(ethylene imine) (PEI) from other groups.[23, 33-34] This is illustrated in Figure 2a, where the transfer curve (I_{ds}-V_{gs}) after PVA exposure exhibits a shift of the neutrality point to more negative gate voltages under ambient conditions. In Figure 2a, our as-transferred graphene FETs show p-type transport behavior with highly positive Dirac points of > 40 V. The neutrality point of as-grown graphene device was a surpassing position gate voltage range, for instance, from -100 to 100 V because the as-grown graphene was heavily p-type doped, as shown in Figure S2 in

the Supporting Information. The reason is that the adsorption of water molecules or/and oxygen can affect the electrical properties of graphene.[22] The intrinsic Fermi level of graphene is downshifted to the valence band when graphene is exposed readily to ambient air. Initially, the Dirac point of the graphene transistors is shifted around 5 V after as-coated graphene devices and then the Dirac voltage was shifted considerably to negative voltages, indicating the n-type doping effect of coated PVA film on monolayer graphene. The current level was reduced with ambipolar behavior. The Dirac point of the doped graphene transistors was shifted significantly from > 40 V to about -20 V after seven days. A 10 wt% doped graphene device was left under ambient conditions for one month, and its Dirac voltage move to positive gate voltage but the n-type doping behavior was still preserved, as shown in Figure 2a. The air stability of a PVA-doped graphene transistor was monitored by measuring the performance as a function of time, in which graphene was doped with a solution concentration of 10 wt% PVA and monitored for more than 30 days, as shown in Figure 2b. After more than 30 days, the Dirac point of these graphene devices that we kept in ambient air was not shifted to over 0 V and exhibited ambipolar behavior, indicating that the doping with PVA was still effective in air to donate electrons to the unintentional p-doping of graphene and recover its expected ambipolar behavior for pristine graphene. The doping-induced electric transport asymmetry shown in Figure 2a is caused by a combination of the neutrality point misalignment at the electrode/channel interface and the variable density of states of the graphene electrodes.[34]

We find that hardening temperature is another factor that can affect the electron transport behavior of graphene FETs using 10 wt% PVA solution. As shown in Figure 3a, similar heavily p-type unipolar to ambipolar conversions were observed when using different baking temperature. The Dirac point of a graphene device changes as temperature increases, for instance, the

corresponding transfer curves (I_{ds}-V_{gs}) of graphene FETs are gradually shifted from 24 V when hardened at 80 ^{o}C to -7 V when hardened at 150 ^{o}C. Figures 3b and 3 c show the Dirac point shift as a function of temperature with a standard deviation and resistance of graphene from source-drain current modulation with various temperatures, respectively. We can also straightforwardly tune the Fermi level of the graphene using coated PVA films with different hardening time, as shown in Supporting Information Figures S3a-f. The Dirac point of PVA-doped graphene transistors initially induced a down-shift compared to that of the as-grown graphene, and then saturated as the baking time increased. Our results show that the hardening temperature and time can control the Dirac point of graphene devices. Figures S3a-f depict devices with or without coating polymer films on graphene, which show the I_{ds}-V_{ds} characteristics that can be interpreted as doped graphene. The transfer characteristics of GFETs were linear before doping. In case of 10 wt% PVA, the total resistance including contact and channel increases to 4.6 kΩ from 1.9 kΩ due to the reduction of carrier concentration in PVA-doped graphene devices in Figure S4a. A shift of the Fermi level owing to charge transfer significantly affects the carrier density in graphene.

To estimate ability of PVA to donate electrons to graphene, we compared the Dirac point shifts between graphene devices based on PVA solutions with different concentrations. Because PVA consists of anion-rich groups, which bear presumably a lone pair of electrons, we considered anion molecules adsorbed on graphene. Electron carriers from these sites are pulled into the graphene monolayer by the downward electric field induced by a back-gate voltage, resulting in a sudden increase in electron density and hence increased conductance. Prior to PVA coating, we first confirmed the transfer characteristics and Raman spectroscopy of all as-grown graphene were the quality and doping level. As the extension of PVA concentration, the neutrality point of graphene device is readily shifted to negative gate voltage, i.e., n-type electrical switching behavior, because

of electron transfer to graphene from coated polymer films. The I_{ds}-V_{gs} curves from low concentration solutions (1 wt%) of PVA-doped graphene devices do not significantly change when compared with that of pristine graphene transistors as shown in Figure 4a. This may be the reason the p-type carrier is compensated by a light n-doping, resulting in the reduction of drain current observed in Figure 4a. On the other hand, there was no appreciable n-dopant remaining at the low concentration of 1 wt%. This will be discussed in more detail later. The transfer characteristics of high concentration solutions (20 wt%) of PVA-coated graphene devices convert to n-type from p-type behaviors as shown in Figure 4b, respectively.

To confirm the n-type doping effect of PVA on as-grown graphene films and derive a better understanding of the interfacial electron transfer, we obtained Raman spectra from these graphene FETs. We characterized both the as-transferred and doped graphene films with different concentration solutions of PVA and compared their Raman spectra features. The G-band and G'-band positions of as-grown graphene are ~1584 cm^{-1} and ~2688 cm^{-1}, respectively.[35] Previous reports for in situ Raman measurements using gate tuning of Dirac points found that the G-band position of graphene upshifts for both n-type and p-type doping.[36-37] On the other hand, the G'-band downshifts with heavy electron donation, and the G'- to G-band intensity ratio has a strong dependence on the doping level. As to our graphene devices, the as-grown graphene shows a slight upshift of G-band position due to unintentional p-type doping by oxygen and other impurities during the transfer process (Figures 5a and 5b). After doping with a low concentration solution of PVA, the graphene G-band starts to downshift to lower wavenumbers, indicating a doping effect that is consistent with the observed conversion from p-type to ambipolar behavior. As the PVA concentration increases, the G-band position upshifts as the graphene FET becomes n-type, which was also observed for doping by gate tuning. The evolution of the G-band FWHM is opposite to

that of the G-band position, which exhibits a narrowing for both electron and hole doping. Furthermore, the change in G'-band position is smaller than that in G-band position, as shown in Figure 5c. Another important parameter to estimate the doping level is the intensity ratio of G' to G-band. $I_{G'}$ to I_G exhibits a strong dependence on the PVA doping concentration as shown in Figure 5d. As PVA concentration increased, PVA peaks were clearly observed at 1362 cm^{-1} and 1441 cm^{-1}.[38] The transfer characteristics of as-grown graphene and typical PVA-coated graphene devices are shown in Supporting Information Figures S4b and S4c, with higher hole and electron mobilities of ~1116 cm^{2}V^{-1}s^{-1} and ~850 cm^{2}V^{-1}s^{-1} compared with as-grown graphene FETs (hole mobility of ~397 cm^{2}V^{-1}s^{-1}), calculated from the transfer curves (I_{ds}-V_{gs}). The field-effect mobilities of electrons and holes were derived from the slope of the source-drain current variation from gate voltage to the linear regime using the equation $\mu = \frac{L_c}{WCV_d}\frac{\Delta I_{ds}}{\Delta V_{gs}}$. Here L_c and W are the channel length and width, $\frac{\Delta I_{ds}}{\Delta V_{gs}}$ is the transconductance, C is the gate capacitance, and V_d is the source-drain voltage. The hole mobility for 10 wt% PVA-coated graphene devices (2200 cm^{2}V^{-1}s^{-1}) showed ~2 times that of the pristine FET (1260 cm^{2}V^{-1}s^{-1}). It has been reported that n-type doping on graphene by the amine groups improves or recovers the electrical properties of graphene.[39-40] The anion in the PVA film donates similarly its lone pair electron to graphene which increases the electron carrier density and induces n-type doping. The charge compensates the p-type doping to recover the intrinsic electrical properties of the as-grown graphene and induces improved charge carrier mobility. Both type conversion and the changed mobilities are reproducible in many graphene FETs that were independently prepared, as shown in Figure S5a and S5b. The V_{gs} dependent carrier density n calculated from the intrinsic mobility of CVD graphene is shown in Figure S5c. The intrinsic mobility of graphene FETs was derived from $\mu_i = 1/n_i e \rho_{xx}$. In the case of PVA-doped graphene FET, the carrier concentration was derived from $n_{PVA} = \sigma/e\mu_i$. We can determine the

carrier concentration both n- and p-type as the above step. Figure S5d shows an optical micrograph of graphene FETs fabricated by e-beam lithography.

Electronic properties of graphene can be adjusted by the chemical modification.[22] However, one drawback of chemical doping is the return of an n-type FET to p-type when exposed to air because the dopants are readily oxidized and lose their ability for n-type doping. For instance, graphene FETs doped with inorganic (NO_2)[41] and organic molecules (amines)[34] exhibit n-type behavior in vacuum, but readily change to a p-type behavior on exposure to air. PEI, which contains an amine group, leads to doped graphene FETs that exhibit n-type behavior with a relatively high on/off ratio, but again changes back to p-type under ambient conditions. The 10 wt% PVA-coated graphene FETs results in n-type characteristics that is stable under ambient air conditions for one month, as shown in Figures 2a and 2b. To assess device stability, we doped graphene FETs with medium concentration (10 wt%) and high concentration (20 wt%) solutions of PVA, and then left the devices under ambient conditions for up to 3 months. The device doped with 10 wt% PVA solution returned to p-type characteristics (similar to as-grown graphene device) as shown in Figure 6a. However, after heat treatment of the sample at 150 ^{o}C for 30 min, the device fully recovered the n-type behavior (Figure 6b). This remarkable reversibility can be attributed to charge transfer as well as the passivation layer by the PVA film, which prevents ambient gases from being adsorbed onto the graphene surface. Although water molecules are adsorbed into the PVA films as time passes, these molecules can be removed by heat treatment. In Figure 6c, the corresponding I_{ds}-V_{gs} characteristics of a device doped with 20 wt% PVA were slightly reduced, but n-type doping behavior was maintained under ambient conditions for up to three months. This high stability in PVA allows the fabrication of circuits using conventional lithography under ambient

conditions. It is expected that this reversible stability will prove beneficial in many aspects of device fabrication in the future.

Conclusion

In summary, we demonstrate a method of implementing n-type doping of as-grown graphene in ambient conditions using solution-based PVA coating. Varying the temperature and hardening time of PVA coated on graphene films can affect the extent of n-type doping level. Furthermore, the graphene FETs can be converted from p-type transport behavior to ambipolar and n-type transport behavior by PVA doping with different concentration solutions. We also demonstrate long-term stability of the n-doped graphene transistors, up to three months in ambient conditions. The highly stable n-doping originates from molecular charge transfer doping and PVA films act as a passivation layer against p-doping from chemical species in the ambient environment. We believe our approach will improve the long-term stability of doped graphene FETs, further enabling us to fabricate basic logic circuits that are stable under ambient conditions.

ACKNOWLEDGMENT

A part of this work was financially supported by Grants-in-Aid for Scientific Research (22226006, 25630063, 25107002) and IRENA Project by JST-EC DG RTD, Strategic International Collaborative Research Program, SICORP. We also acknowledge supports from Center for Nano Lithography & Analysis (The University of Tokyo) supported by 'Nanotechnology Platform'

(project No. 12024046) of MEXT, Japan. A part of this work was also supported by 'Global Center for Excellence for Mechanical Systems Innovation' (The University of Tokyo); and VLSI Design and Education Center (VDEC), The University of Tokyo, in collaboration with Cadence Corporation.

Supporting Information Available: Raman spectra of as-grown graphene and **c**omparison of as-transferred graphene and doped graphene including device performance. Figure S1-S5. This material is available free of charge via the Internet at http://pubs.acs.org.

Figure 1. (a) SEM image of as-grown graphene on a copper substrate grown via ACCVD. (b) Intensity ratio of G'- to G-band of scanning Raman spectroscopy using an excitation energy of 514.5 nm (2.41 eV). (c) Schematic illustration of polymer-films-coated graphene field-effect transistors with source, drain, and gate electrodes. (d) Corresponding SEM image of graphene transferred onto SiO_2/Si substrate (600 nm thick oxide layer) between the source/drain electrodes (channel length = 5 μm, width = 20 μm).

Figure 2. Corresponding electronic transport properties of 10 wt% PVA-treated graphene devices. (a) Stability of transfer characteristics of 10 wt% PVA graphene devices as a function of time evaluation under ambient conditions (channel length = 20 μm, width = 10 μm, V_{ds} = -10 mV). (b) Dirac point shift of the 10 wt% PVA-coated graphene transistors in terms of assessment time under ambient conditions.

Figure 3. Electronic properties of PVA-doped graphene transistors (channel length = 10 μm, width = 10 μm). (a) Corresponding I_{ds}-V_{gs} characteristics of 10 wt% PVA-coated graphene devices as a function of different hardening temperature for 10 min. (b) Dirac point position shift of graphene

transistors depend on diverse hardening temperature with standard deviation. (c) Resistance of graphene depending on different hardening temperature.

Figure 4. Comparisons of electronic properties between high concentration (20 wt%) PVA-treated CVD graphene transistors and low concentration (1 wt%) PVA-treated devices. (a) Corresponding transfer (I_{ds}-V_{gs}) characteristics of as-grown and low concentration solution of PVA-doped graphene devices as a function of gate voltage before and after doping, respectively. (b) Corresponding transfer curves of as-grown and high concentration solution (20 wt%) of PVA-doped graphene transistors as a function of gate voltage before and after doping, respectively.

Figure 5. (a) Raman spectra of monolayer graphene doped with various concentration solutions of PVA on a SiO_2/Si substrate. The intensity of G'- to G-band ratio of as-grown graphene was > 2, while the peak position of G- and G'-bands are ~1585 cm^{-1} and ~2688 cm^{-1}. The stars indicate the Raman features from the PVA films. (b) G-band position shift and its FWHM in terms of PVA concentration, respectively. (c) G'-band position shift of monolayer graphene as a function of PVA concentrations. (d) Intensity of G'- to G-band ratio as a function of various concentration solutions of PVA.

Figure 6. Long-term stability of n-type doping. (a) Corresponding I_{ds}-V_{gs} characteristics of as-grown, as-doped (10 wt%), and after 104 days of graphene transistors under ambient air conditions, respectively. (b) Corresponding I_{ds}-V_{gs} characteristics of lightly doped (10 wt%) graphene devices after 104 days and after re-heat treatment at 150 ^{o}C. (c) Stability of I_{ds}-V_{gs} characteristics of 20 wt% PVA-doped graphene devices after 63 days, 90 days, and 104 days, respectively.

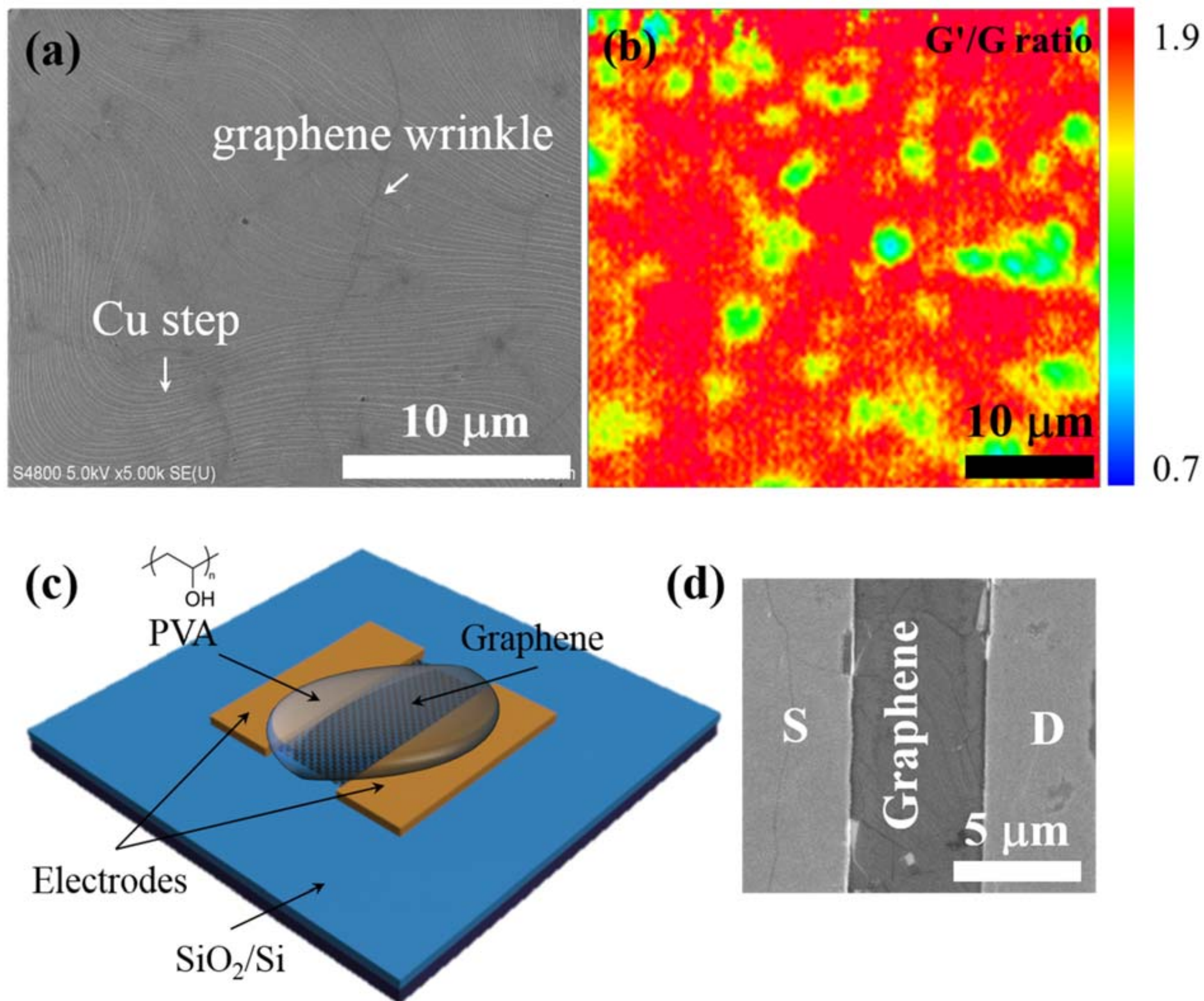

Figure 1. Kim et al.

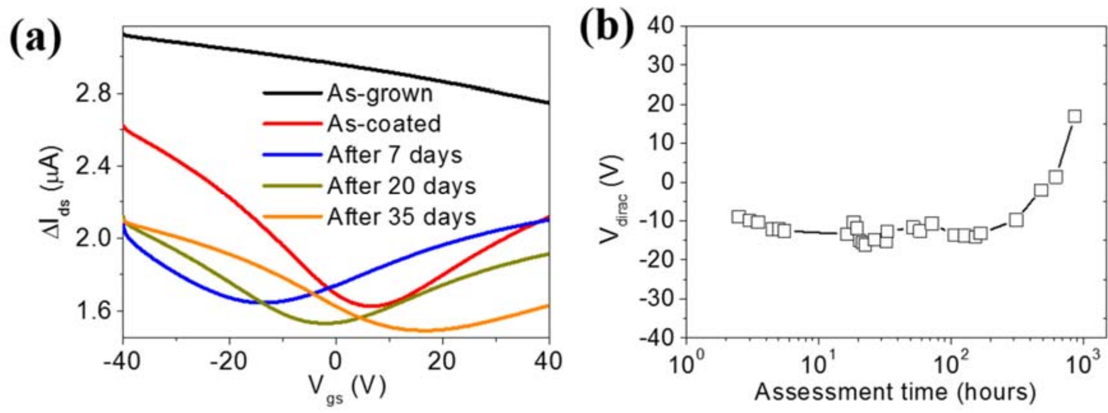

Figure 2. Kim et al.

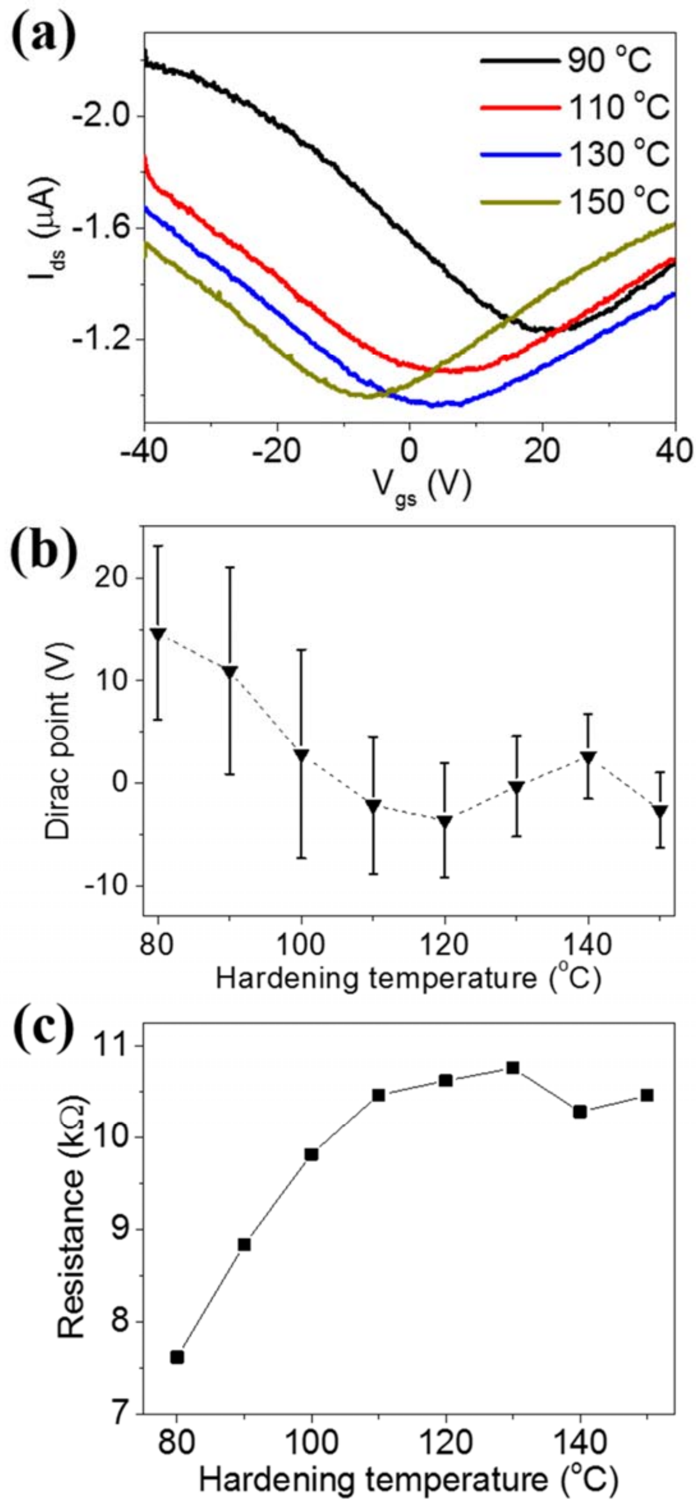

Figure 3. Kim et al.

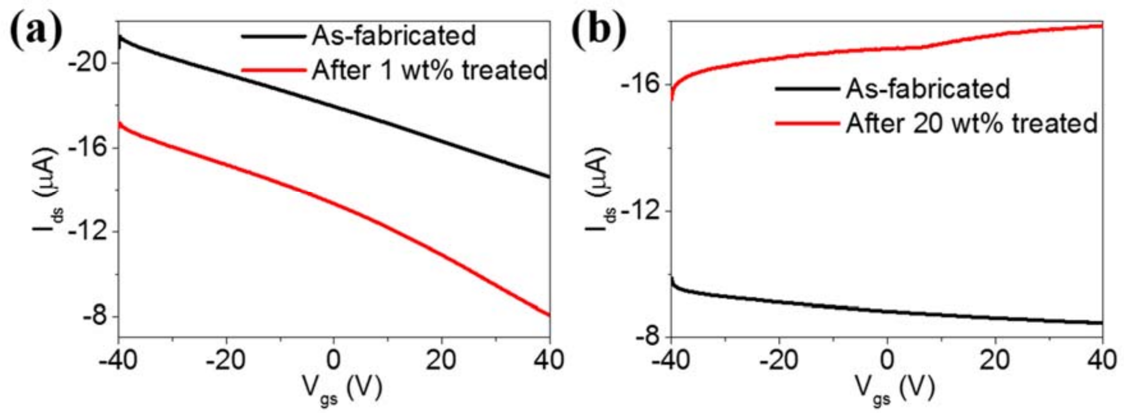

Figure 4. Kim et al.

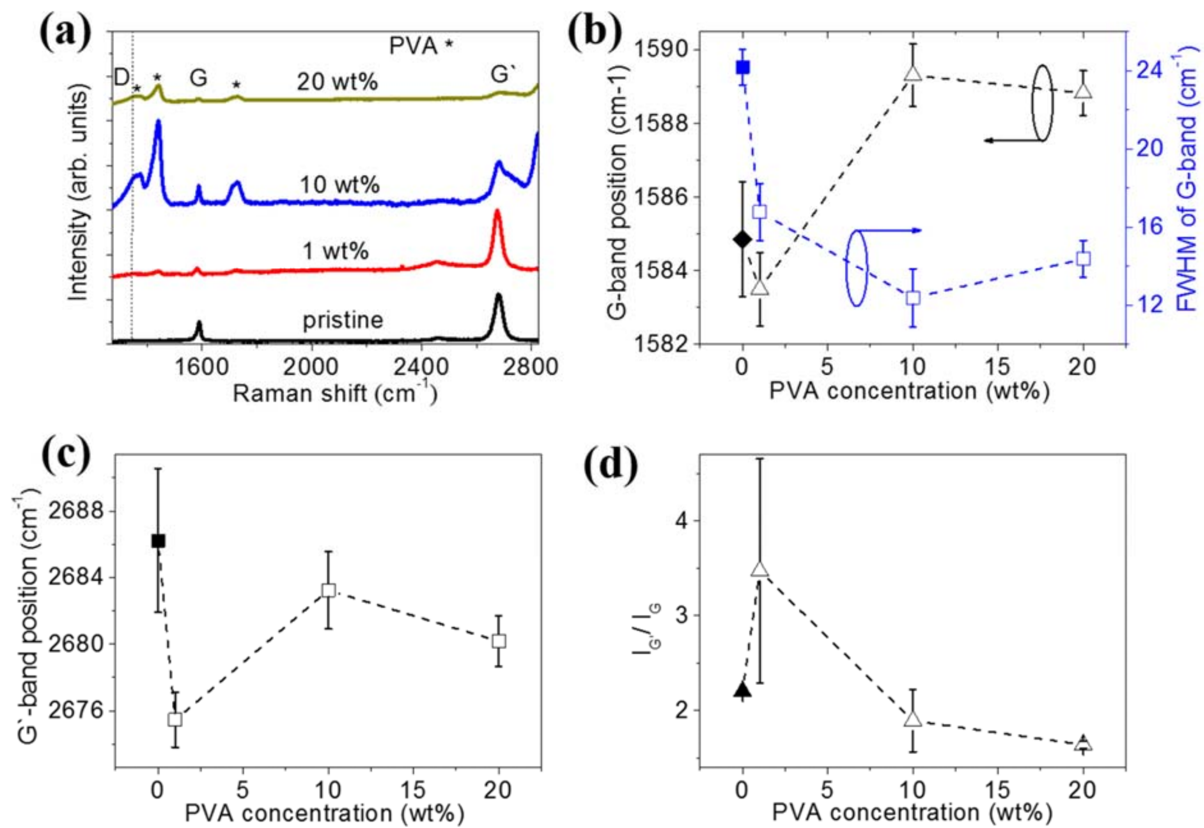

Figure 5. Kim et al.

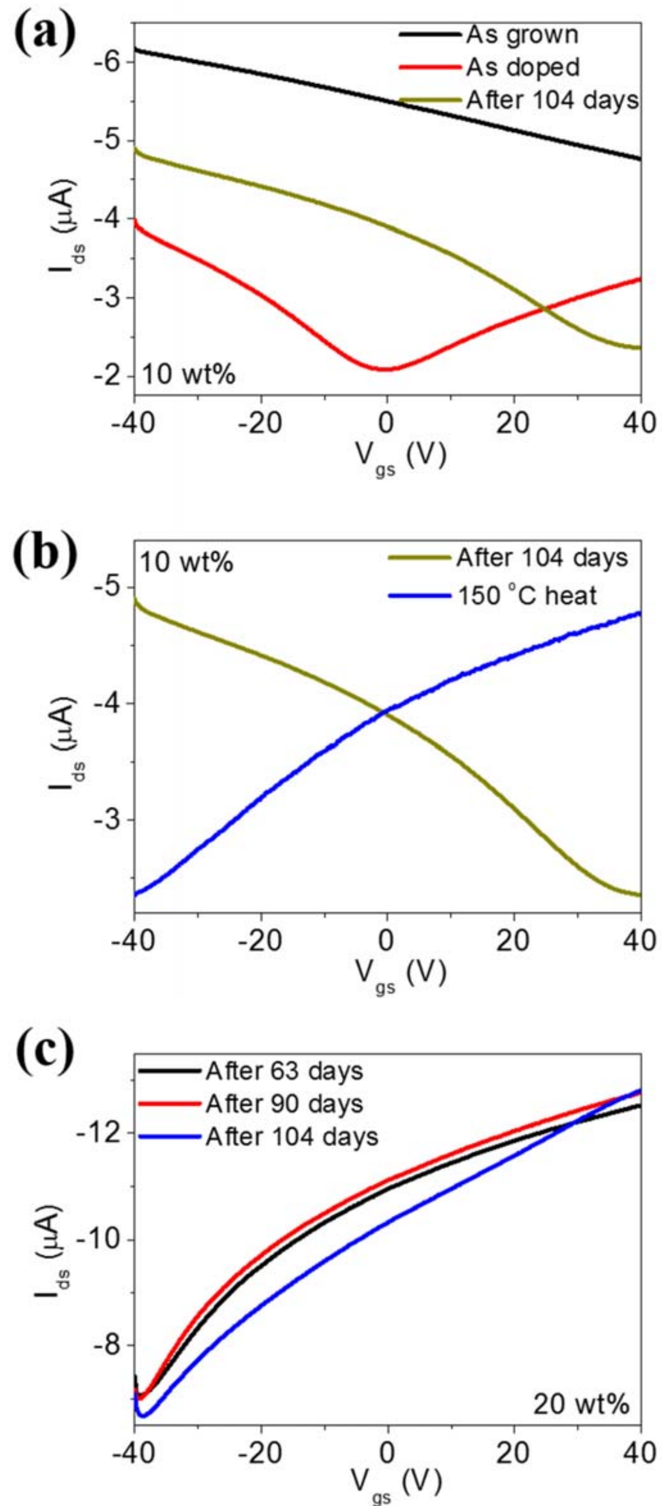

Figure 6. Kim et al.

REFERENCES

1. Avouris, Ph.; Chen, Z.; Perebeinos, V. Carbon-Based Electronics. *Nat. Nanotechnol.* **2007**, 2, 605–615.

2. Geim, A. K.; Novoselov, K. S. The Rise of Graphene. *Nat. Mater.* **2007**, 6, 183–191.

3. Novoselov, K. S.; Fal'ko, V. I.; Colombo, L.; Gellert, P. R.; Schwab, M. G.; Kim, K. A Roadmap for Graphene. *Nature* **2012**, 490, 192–200.

4. Morozov, S. V.; Novoselov, K. S.; Katsnelson, M. I.; Schedin, F.; Elias, D. C.; Jaszczak, J. A.; Geim, A. K. Giant Intrinsic Carrier Mobilities in Graphene and Its Bilayer. *Phys. Rev. Lett.* **2008**, 100, 016602.

5. Du, X.; Skachko, I.; Barker, A.; Andrei, E. Y. Approaching Ballistic Transport in Suspended Graphene. *Nat. Nanotechnol.* **2008**, 3, 491–495.

6. Du, X.; Skachko, I.; Duerr, F.; Luican, A.; Andrei, E. Y. Fractional Quantum Hall Effect and Insulating Phase of Dirac Electrons in Graphene. *Nature* **2009**, 462, 192–195.

7. Bolotin, K. I.; Ghahari, F.; Shulman, M. D.; Stormer, H. L.; Kim, P. Observation of The Fractional Quantum Hall Effect in Graphene. *Nature* **2009**, 462, 196–199.

8. Lee, C.; Wei, X.; Kysar, J. W.; Hone, J. Measurement of The Elastic Properties and Intrinsic Strength of Monolayer Graphene. *Science* **2008**, 321, 385–388.

9. Han, M. Y.; Özyilmaz, B.; Zhang, Y.; Kim, P. Energy Band-Gap Engineering of Graphene Nanoribbons. *Phys. Rev. Lett.* **2007**, 98, 206805.

10. Chen, Z.; Lin, Y.-M.; Rooks, M. J.; Avouris, Ph. Graphene Nano-Ribbon Electronics. *Phys. E* **2007**, 40, 228–232.

11. Li, X.; Wang, X.; Zhang, L.; Lee, S.; Dai, H. Chemically Derived, Ultrasmooth Graphene Nanoribbon Semiconductors. *Science* **2008**, 319, 1229–1232.

12. Wang, X.; Ouyang, Y.; Li, X.; Wang, H.; Guo, J.; Dai, H. Room-Temperature All-Semiconducting Sub-10-nm Graphene Nanoribbon Field-Effect Transistors. *Phys. Rev. Lett.* **2008**, 100, 206803.

13. Ohta, T.; Bostwick, A.; Seyller, T.; Horn, K.; Rotenberg, E. Controlling The Electronic Structure of Bilayer Graphene. *Science* **2006**, 313, 951–954.

14. Castro, E. V.; Novoselov, K. S.; Morozov, S. V.; Peres, N. M. R.; Lopes dos Santos, J. M. B.; Nilsson, J.; Guinea, F.; Geim, A. K.; Castro Neto, A. H. Biased Bilayer Graphene: Semiconductor with a Gap Tunable by the Electric Field Effect. *Phys. Rev. Lett.* **2007**, 99, 216802.

15. Xia, F.; Farmer, D. B.; Lin, Y.-M.; Avouris, Ph. Graphene Field-Effect Transistors with High On/Off Current Ratio and Large Transport Band Gap at Room Temperature. *Nano Lett.* **2010**, 10, 715–718.

16. Zhang, Y.; Tang, T.-T.; Girit, C.; Hao, Z.; Martin, M. C.; Zettl, A.; Crommie, M. F.; Ron Shen, Y.; Wang, F. Direct Observation of a Widely Tunable Bandgap in Bilayer Graphene. *Nature* **2009**, 459, 820–823.

17. Bai, J.; Zhong, X.; Jiang, S.; Huang, Y.; Duan, X. Graphene Nanomesh. *Nat. Nanotechnol.* **2010**, 5, 190–194.

18. Levesque, P. L.; Sabri, S. S.; Aguirre, C. M.; Guillemette, J.; Siaj, M.; Desjardins, P.; Szkopek, T.; Martel, R. Probing Charge Transfer at Surfaces Using Graphene Transistors. *Nano Lett.* **2011**, 11, 132–137.

19. Castro Neto, A. H.; Guinea, F.; Peres, N. M. R.; Novoselov, K. S.; Geim, A. K. The Electronic Properties of Graphene. *Rev. Mod. Phys.* **2009**, 81, 109–162.

20. Dong, X.; Fu, D.; Fang, W.; Shi, Y.; Chen, P.; Li, L.-J. Doping Single-Layer Graphene with Aromatic Molecules. *Small* **2009**, 5, 1422–1426.

21. Guo, B.; Liu, Q.; Chen, E.; Zhu, H.; Fang, L.; Gong, J. R. Controllable N-Doping of Graphene. *Nano Lett.* **2010**, 10, 4975–4980.

22. Schedin, F.; Geim, A. K.; Morozov, S. V.; Hill, E. W.; Blake, P.; Katsnelson, M. I.; Novoselov, K. S. Detection of Individual Gas Molecules Adsorbed on Graphene. *Nat. Mater.* **2007**, 6, 652–655.

23. Yan, Z.; Yao, J.; Sun, Z.; Zhu, Y.; Tour, J. M. Controlled Ambipolar-to-Unipolar Conversion in Graphene Field-Effect Transistors Through Surface Coating with Poly(ethylene imine)/Poly(ethylene glycol) films. *Small* **2012**, 8, 59–62.

24. Li, X.; Tang, T.; Li, M.; He, X. Photochemical Doping of Graphene Oxide Thin Films with Nitrogen for Electrical Conductivity Improvement. *J. Mater. Sci.: Mater. Electron.* **2015,** *26*, 1770–1775.

25. Wang, X.; Sun, G.; Routh, P.; Kim, D.-H.; Huang, W.; Chen, P. Heteroatom-doped Graphene Materials: Syntheses, Properties and Applications. *Chem. Soc. Rev.* **2014**, 43, 7067–7098.

26. Li, X.; Tang, T.; Li, M.; He, X. Nitrogen-doped Graphene Films from Simple Photochemical Doping for n-type Field-Effect Transistors. *Appl. Phys. Lett.* **2015,** 106, 013110.

27. Chen, J.-H.; Jang, C.; Adam, S.; Fuhrer, M. S.; Williams, E. D.; Ishigami, M. Charged-Impurity Scattering in Graphene. *Nat. Phys.* **2008**, 4, 377–381.

28. Zhao, P.; Kumamoto, A.; Kim, S.; Chen, X.; Hou, B.; Chiashi, S.; Einarsson, E.; Ikuhara, Y.; Maruyama, S. Self-Limiting Chemical Vapor Deposition Growth of Monolayer Graphene from Ethanol. *J. Phys. Chem. C* **2013**, 117, 10755–10763.

29. Li, X.; Cai, W.; An, J.; Kim, S.; Nah, J.; Yang, D.; Piner, R.; Velamakanni, A.; Jung, I.; Tutuc, E.; Banerjee, S. K.; Colombo, L.; Ruoff, R. S. Large-Area Synthesis of High-Quality and Uniform Graphene Films on Copper Foils. *Science* **2009**, 324, 1312–1314.

30. Malard, L. M.; Pimenta, M. A.; Dresselhaus, G.; Dresselhaus, M. S. Raman Spectroscopy in Graphene. *Phys. Rep.* **2009**, 473, 51–87.

31. Peng, X.; Horowitz, G.; Fichou, D.; Garnier, F. All-Organic Thin-Film Transistors made of Alpha-Sexithienyl Semiconducting and Various Polymeric Insulating Layers. *Appl. Phys. Lett.* **1990**, 57, 2013–2015.

32. Swiggers, M. L.; Xia, G.; Slinker, J. D.; Gorodetsky, A. A.; Malliaras, G. G.; Headrick, R. L.; Weslowski, B. T.; Shashidhar, R. N.; Dulcey, C. S. Orientation of Pentacene Films Using Surface Alignment Layers and Its Influence on Thin-Film Transistor Characteristics. *Appl. Phys. Lett.* **2001**, 79, 1300–1302.

33. Aikawa, S.; Einarsson, E.; Thurakitseree, T.; Chiashi, S.; Nishikawa, E.; Maruyama, S. Deformable Transparent All-Carbon-Nanotube Transistors. *Appl. Phys. Lett.* **2012**, 100, 063502.

34. Farmer, D. B.; Golizadeh-Mojarad, R.; Perebeinos, V.; Lin, Y.-M.; Tulevski, G. S.; Tsang, J. C.; Avouris, Ph. Chemical Doping and Electron-Hole Conduction Asymmetry in Graphene Devices. *Nano Lett.* **2009**, 9, 388–392.

35. Ferrari, A. C.; Meyer, J. C.; Scardaci, V.; Casiraghi, C.; Lazzeri, M.; Mauri, F.; Piscanec, S.; Jiang, D.; Novoselov, K. S.; Roth, S.; Geim, A. K. Raman Spectrum of Graphene and Graphene Layers. *Phys. Rev. Lett.* **2006**, 97, 187401.

36. Pisana, S.; Lazzeri, M.; Casiraghi, C.; Novoselov, K. S.; Geim, A. K.; Ferrari, A. C.; Mauri, F. Breakdown of The Adiabatic Born-Oppenheimer Approximation in Graphene. *Nat. Mater.* **2007**, 6, 198–201.

37. Das, A.; Pisana, S.; Chakraborty, B.; Piscanec, S.; Saha, S. K.; Waghmare, U. V.; Novoselov, K. S.; Krishnamurthy, H. R.; Geim, A. K.; Ferrari, A. C.; Sood, A. K. Monitoring Dopants by Raman Scattering in an Electrochemically Top-gated Graphene Transistor. *Nat. Nanotechnol.* **2008**, 3, 210–215.

38. Thomas, P. S.; Stuart, B. H. A Fourier Transform Raman Spectroscopy Study of Water Sorptin by PVA. *Spectrochim. Acta, Part A* **1997**, 53, 2275–2278.

39. Yan, Z.; Sun, Z.; Lu, W.; Yao, J.; Zhu, Y.; Tour, J. M. Controlled Modulation of Electronic Properties of Graphene by Self-Assemble Monolayers on SiO_2 Substrates. *ACS Nano* **2011**, 5, 1535–1540.

40. Suk, J. W.; Lee, W. H.; Lee, J.; Chou, H.; Piner, R. D.; Hao, Y.; Akinwande, D.; Ruoff, R. S. Enhancement of the Electrical Properties of Graphene Grown by Chemical Vapor Deposition via Controlling the Effects of Polymer Residue. *Nano Lett.* **2013**, 13, 1462–1467.

41. Williams, J. R.; Dicarlo, L.; Marcus, C. M. Quantum Hall Effect in a Gate-Controlled p-n Junction of Graphene. *Science* **2007**, 317, 638–641.

Table of Contents Graphic

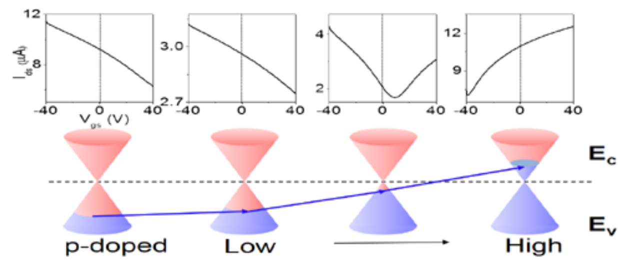

Supporting Information

Highly Stable and Tunable n-Type Graphene Field-Effect Transistors with Poly(vinyl alcohol) Films

Sungjin Kim[†], Pei Zhao[§], Shinya Aikawa[‡], Erik Einarsson[⊥], Shohei Chiashi[†], and Shigeo Maruyama[*,†#]

[†]Department of Mechanical Engineering, The University of Tokyo, 7-3-1 Hongo, Bunkyo-ku, Tokyo 113-8656, Japan

[§]Institute of Applied Mechanics, Zhejiang University, Hangzhou, Zhejiang 310027, China

[‡]Research Institute for Science and Technology, Kougakuin University, 2665-1 Nakano, Hachioji, Tokyo 192-0015, Japan

[⊥]Department of Electrical Engineering, University at Buffalo, New York 14260-2500, United States

[#]Energy NanoEngineering Laboratory, National Institute of Advanced Industrial Science and Technology (AIST), 1-2-1 Namiki, Tsukuba, 305-8564, Japan

Corresponding Author

[*]E-mail: maruyama@photon.t.u-tokyo.ac.jp

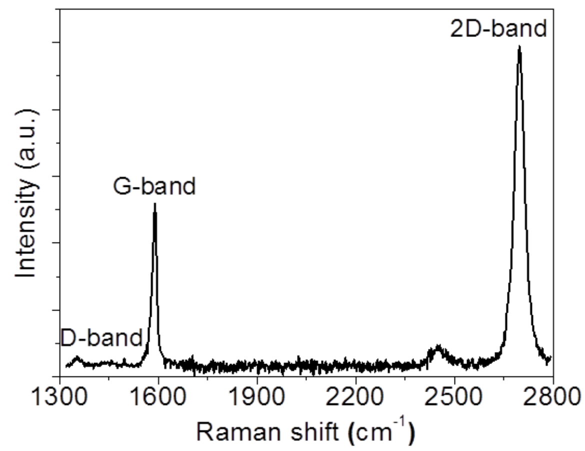

Figure S1. Raman spectroscopy using an excitation energy of 488 nm (2.54 eV) for as-grown graphene on SiO_2/Si substrate.

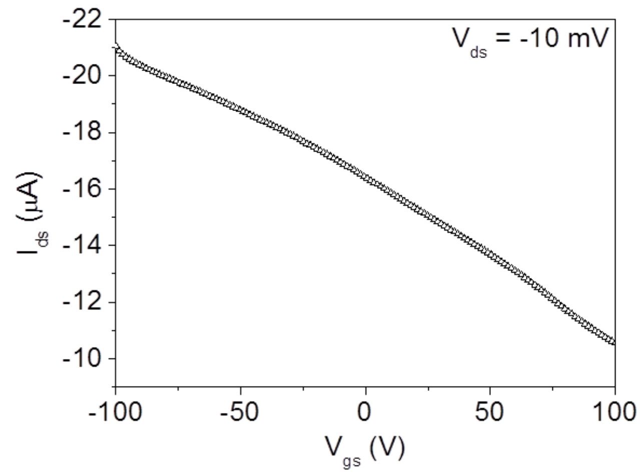

Figure S2. Corresponding transfer characteristics of as-grown graphene device**.**

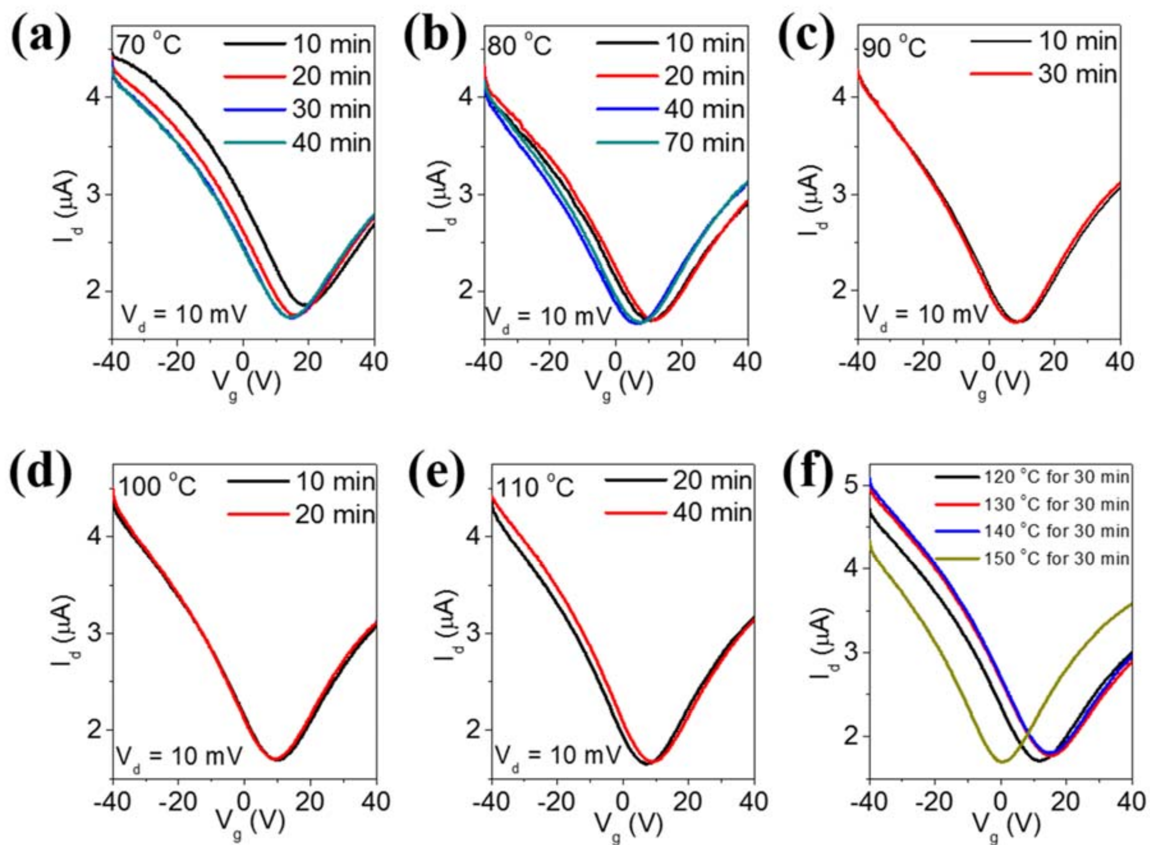

Figure S3. (a) - (f) I_{ds}-V_g characteristics of 10 wt % PVA-doped graphene transistors with different baking temperature and time.

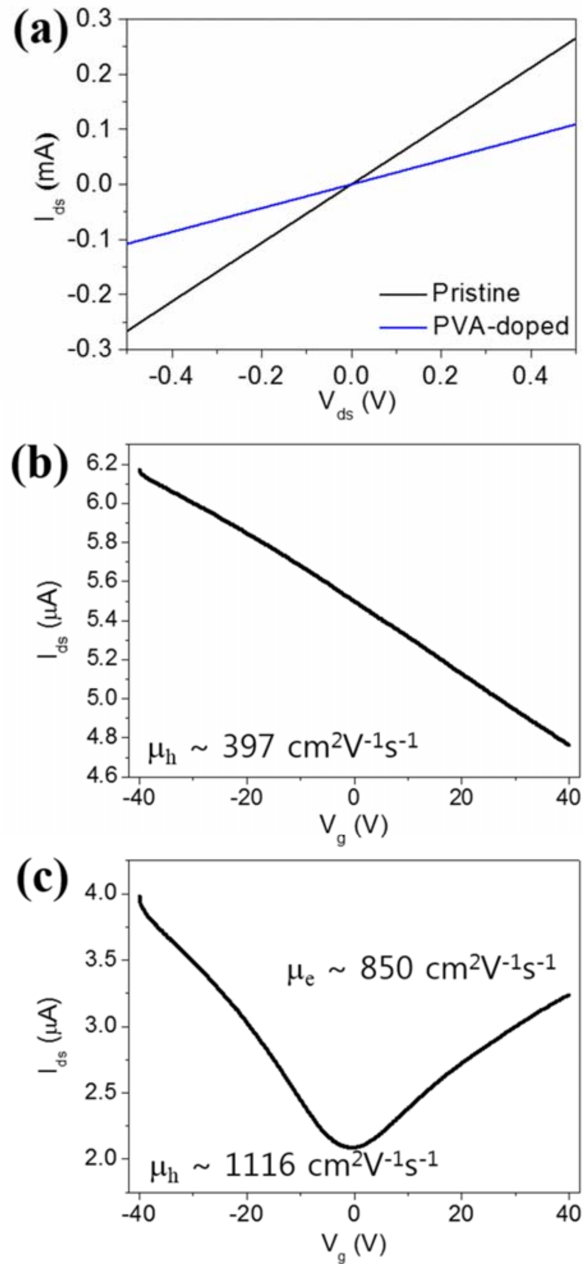

Figure S4. I_{ds}-V_g characteristics before and after 10 wt % PVA-coated graphene devices under ambient conditions (V_{ds} = -10 mV). (a) I_{ds}-V_{ds} curves before and after PVA doped. (b) Transfer curve for as-grown CVD graphene transistor. (c) Transfer curve for 10 wt % PVA coated graphene devices under ambient air condition.

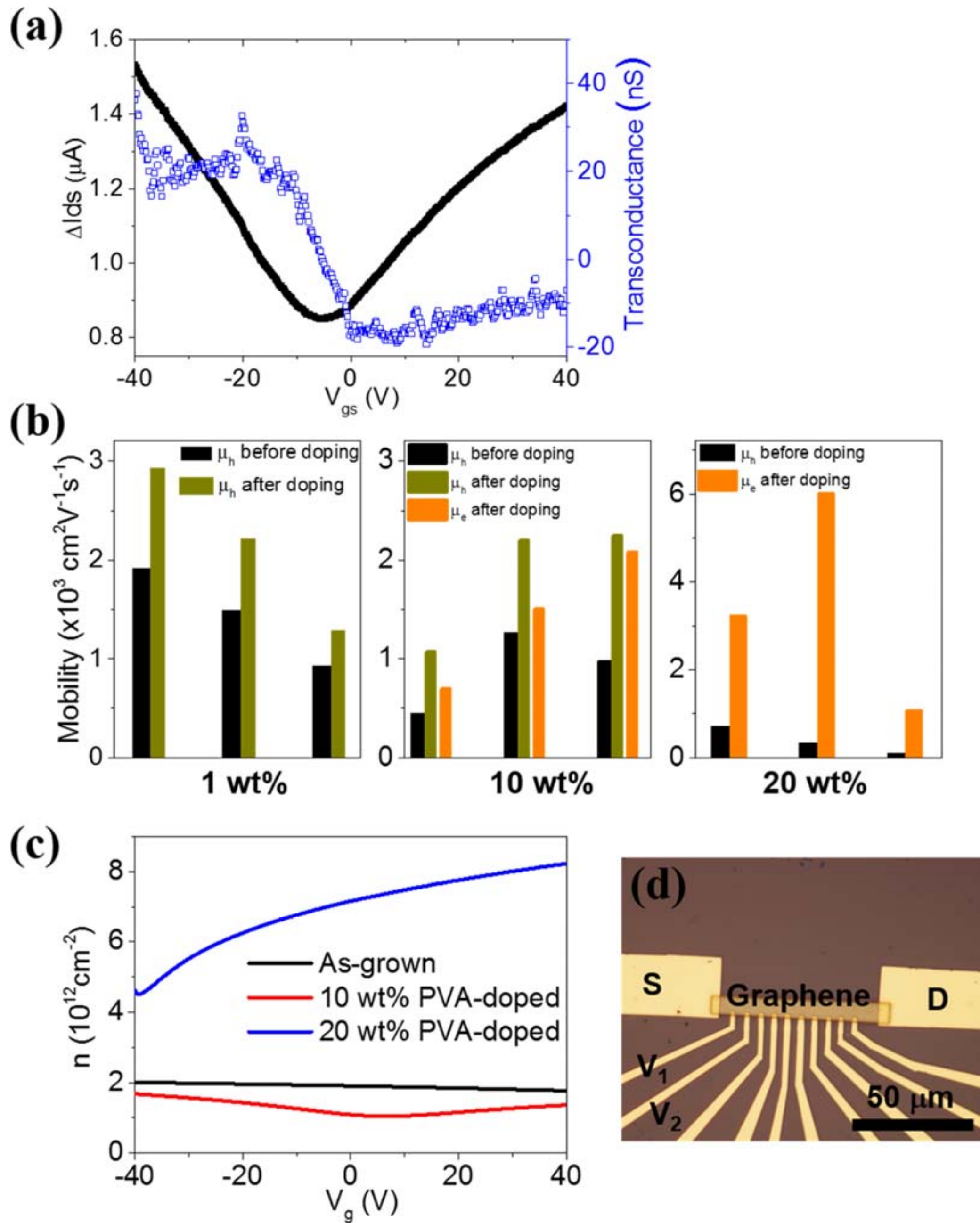

Figure S5. (a) I_{ds}-V_{gs} characteristics and transconductance as a function of gate voltage for 10 wt % PVA-doped graphene transistors (V_{ds} = -10 mV). (b) Mobility before and after 1, 10, and 20 wt % PVA coated graphene devices. (c) Carrier concentration of graphene as a function of gate voltage. (d) Optical microscopy image of the graphene device.